JOURNAL OF MATERIALS SCIENCE **34** (1999) 5961–5974

Factors affecting work of fracture of uPVC film

A. ARKHIREYEVA, S. HASHEMI, M. O'BRIEN
University of North London, School of Polymer Technology, Holloway Road, London N7 8DB, England, UK
E-mail: s.hashemi@unl.ac.uk

Essential work of fracture (EWF) approach was used to evaluate the fracture toughness of uPVC film. It was found that the specific essential work of fracture, (w_e) is independent of specimen width, specimen gauge length, loading rate and test temperature, but dependent on the geometry of the test specimens. Test temperature and geometry were the only testing parameters affecting the specific non-essential work of fracture (βw_p) in a very significant way. The plastic zone shape factor (β) was found to be very sensitive to both the geometry and temperature. It was established that both w_e and βw_p could be partitioned into components that are linked to yielding (i.e. $w_{e,y}$ and $\beta_y w_{p,y}$) and necking/tearing (i.e. $w_{e,nt}$ and $\beta_{nt} w_{p,nt}$) processes. The only testing parameter that affected $w_{e,y}$ was test temperature, whereas $w_{e,nt}$ was affected by test temperature as well as geometry. All testing parameters used in this study affected the values of $\beta_y w_{p,y}$ and $\beta_{nt} w_{p,nt}$.

1. Introduction

Linear Elastic Fracture Mechanics (LEFM) approach is often used to characterise fractures that occur at nominal stresses well below the uniaxial tensile yield stress of a material. Under this condition, plastic flow at the tip of the crack is intimately associated with a fracture process which is brittle in nature. A single fracture parameter such as the Critical Stress Intensity Factor, K_{Ic} or the Critical Strain Energy Release Rate, G_{Ic} have been found to be sufficient to characterise this type of fracture at its critical condition. However, the LEFM approach can not be adopted in characterising the failure of ductile and toughened polymers, where a large plastic zone often exists at the tip of the crack, and, much of the plastic flow work dissipated in this zone is not directly associated with the fracture process. For ductile materials, two approaches have been used in order to characterise the fracture behaviour, namely, the essential work of fracture (EWF) and the J-integral. EWF approach has recently gained popularity due to its experimental simplicity. This approach which was proposed by Broberg [1] assumes that the non-elastic region at the tip of a crack may be divided into two regions: an inner region where the fracture process takes place, and the outer region where the plastic deformation takes place. The total work of fracture can then be partitioned into two components: work that is expended in the inner fracture process zone to form a neck and subsequent tearing, and the work which is consumed by various deformation mechanisms in the surrounding outer plastic deformation zone. The former is referred to as "Essential Work of Fracture" and the latter as "Non-Essential Work of Fracture". The method has been used to study the fracture behaviour of wide range of materials such as metals [2–4], polymer films [e.g. 5–12] and papers [13, 14] under plane-stress conditions. Studies on these materials indicate that the method provides a useful means by which fracture toughness can be determined.

In this study, EWF approach was used to determine the fracture toughness of an uPVC film. The effects of specimen dimensions (i.e. width and gauge length), specimen geometry, loading rate and temperature on EWF parameters for uPVC are investigated in detail.

2. Essential work of fracture (EWF)

This method, was first proposed by Broberg [1] who suggested that when the ultimate failure of the test specimen is preceded by extensive yielding and slow crack growth, a toughness parameter called the Specific Essential Work of fracture (SEWF), w_e which might be considered as a material constant may be evaluated.

EWF approach is based on the assumption that the total work of fracture, W_f is the sum of two energy terms,

$$W_f = W_e + W_p \tag{1}$$

where the first term, W_e, is called the essential work of fracture, which is the energy consumed in the inner fracture process zone (IFPZ), where the actual fracture occurs (see Fig. 1). W_e is therefore a pure crack resistance parameter and thus regarded as fracture toughness. The second term, W_p, which is referred to as the non-essential work or plastic deformation work, is the energy dissipated in the outer plastic deformation zone (OPDZ) as shown in Fig. 1, which for polymers involves microvoiding and shear yielding.

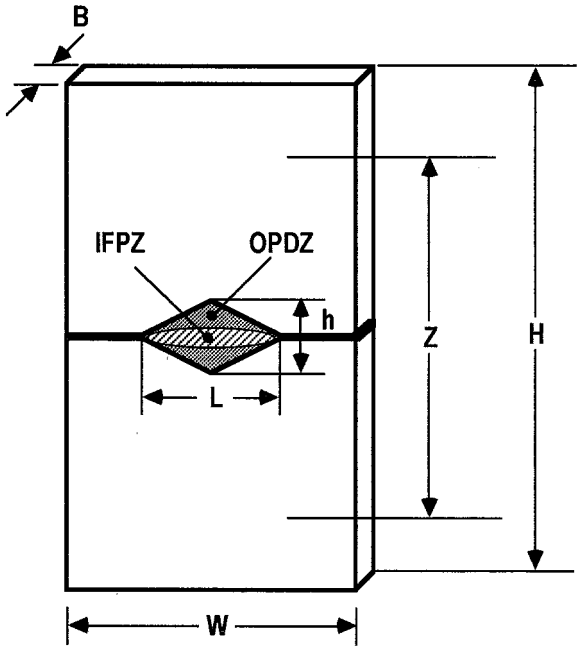

Figure 1 Inner fracture process zone (IFPZ) and outer plastic deformation zone (OPDZ) in a double edge notched tension (DENT) specimen.

Taking into consideration that W_e is surface energy related and W_p is volume related, one may write;

$$w_f = \frac{W_f}{LB} = w_e + \frac{w_p V_p(L, B)}{LB} \tag{2}$$

where $w_e = W_e/LB$, $w_p = W_e/BL^2$ and $V_p(L, B)$ is the volume of the plastic deformation zone. Assuming that the volume of the plastic deformation zone, $V_p(L, B)$ is proportional to BL^2 with a proportionality constant, β, that is independent of the ligament length, we obtain:

$$w_f = w_e + \beta w_p L \tag{3}$$

where w_e is termed the "Specific Essential Work of Fracture (SEWF)" and w_p is termed the "Specific Non-Essential Work of Fracture (SNEWF)".

2.1. Validity of the essential work of fracture

Equation 3 predicts a linear relationship between the specific total work of fracture, w_f and the ligament length, L. To obtain w_e, series of specimens which vary in ligament length are prepared and tested to complete failure. Specimen geometries such as the Double-Edge Notched Tension (DENT) and the Single-Edge Notched Tension (SENT) are commonly used for this purpose. The DENT geometry is generally favoured, as its symmetry prevents the specimen from twisting, which could be a problem for non-symmetrical geometries such SENT, particularly if the specimen is thin and long.

The total area under the load-displacement curve gives the total work of fracture W_f from which the specific total work of fracture, w_f is evaluated. A w_e value is then estimated from the interception of the linear regression of the plot of w_f vs. L as shown in Fig. 2,

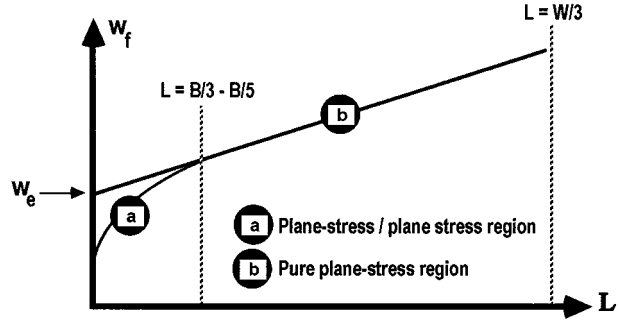

Figure 2 Specific work of fracture versus ligament length, L.

with the w_f axis (i.e. at $L = 0$) as required by Equation 3. The slope of this linear regression line gives βw_p, which is a measure of the specific non-essential work of fracture. For a given material one would expect βw_p to increases with ductility or otherwise approach a value of zero with increasing degree of brittleness. The explicit determination of w_p requires the knowledge of the shape factor β whose value is related to the shape of the plastic zone. For example, volume of a diamond-shaped plastic deformation zone, $V_p(L, B)$ (see Fig. 1) with overall height, h, is related to the ligament length, L, and the shape factor, β, by a simple relationship;

$$V_p(L, B) = \tfrac{1}{2}BLh = \beta BL^2 \tag{4}$$

Equation 4 suggests that a linear relationship exists between the overall height of the plastic deformation zone (h) and the ligament length (L) with a slope of 2β.

It has been suggested [2–4], that the specimen dimensions utilised in measuring w_e should satisfy several pre-requisites in order to achieve linearity between w_f and L. It should be borne in mind that inherent in Equation 3 are the assumptions that (i) the ligament length controls the size of the outer plastic deformation zone (OPDZ) that surrounds the fracture process zone and (ii) the volume of OPDZ is proportional to BL^2 (i.e. Equation 4). This proportionality may be affected in the following ways:

- If the ligament length, L, is not small compared to the total width of the sample, W, then the size of the OPDZ can be disturbed by the lateral boundaries of the specimen. In order to confine plastic deformation to the ligament area, the width restriction of $L \leq W/3$ has been proposed and frequently used.
- If yielding of the ligament length occurs prior to crack growth, then the size of the OPDZ is no longer controlled by the ligament length. In order to ensure that complete yielding of ligament length occurs before crack growth (thereby maintaining the proportionality of W_p and L^2) the plastic zone size restriction of $L \leq 2R_p$ has been proposed, where R_p is the radius of the plastic zone at the crack tip.
- If the ligament length is not too large compared to the thickness of the sample, B, then the state of stress in the ligament region could become that of a plane-strain/plane-stress (i.e. mixed mode stress state) at short ligament lengths, rather than the

required pure plane-stress state. As a result, both w_e and w_p become dependent on L giving rise to a non-linear relationship between w_f and L as illustrated in Fig. 2. This nonlinearity is due to the increasing plastic flow constraint with decreasing ligament length. To prevent the onset of mixed-mode stress state, the thickness restriction of $L \geq 3B - 5B$ has been recommended and adhered to.

Based on the above limitations, the following ligament size restrictions were recommended empirically, for a valid plane-stress determination of w_e;

$$3B - 5B \leq L \leq \min(2R_p, W/3) \tag{5}$$

The size of the plastic zone, $2R_p$, may be estimated from the following linear elastic fracture mechanics equation;

$$2R_p = \frac{1}{\pi}\frac{E w_e}{\sigma_y^2} \tag{6}$$

where E and σ_y are respectively the Young's modulus and the tensile yield stress of the material.

To verify how the state of stress may depend on ligament length, values of the maximum net-section stress, $\sigma_n = P_{max}/LB$ (where P_{max} is the maximum load on the load-displacement curve) are often plotted against ligament length, L. According to plasticity theory [15], if σ_y is the uniaxial yield stress of the material, then, under pure plane stress conditions $\sigma_n = m\sigma_y$ where m is the plastic constraint factor whose value for single edge notched tension specimen is 1.0 and for double edge notched tension specimen is 1.15. The value of m however increases with the decreasing ligament length, as the state of stress in the ligament region changes from one of a pure plane-stress to one of a pure plane strain for which $m = 3$.

2.2. Partitioning of the essential work of fracture

In some materials, including the uPVC polymer studied here, the full ligament yielding of the DENT specimen gives rise to a sudden load drop in the load-displacement diagram, as illustrated in Fig. 3. Based on this load drop, it is possible to distinguish between the specific work of fracture for yielding (w_y) and the specific work of fracture for necking and subsequent fracture (w_{nt}). The specific total work of fracture, w_f may thus be written as:

$$w_f = w_e + \beta w_p L = w_y + w_{nt} \tag{7}$$

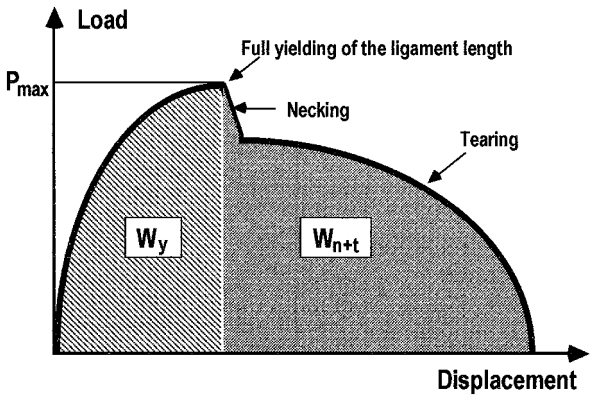

Figure 3 Load-displacement diagram of a DENT specimen showing work of fracture parameters.

Most recently, Karger-Kocsis, et al. [9, 10], demonstrated that w_y and w_{nt} contributions to w_f as a function of ligament length may be expressed as:

$$w_y = w_{e,y} + \beta_y w_{p,y} L \tag{8}$$

$$w_{nt} = w_{e,nt} + \beta_{nt} w_{p,nt} L \tag{9}$$

where $w_{e,y}$ and $w_{e,nt}$ represent the specific essential work of fracture for yielding and necking/tearing respectively. $\beta_y w_{p,y}$ and $\beta_{nt} w_{p,nt}$ represent their respective non-essential work of fracture.

2.3. Estimation of the essential work of fracture via crack-opening-displacement (COD)

It has been shown [2, 6–8] that a reasonable estimate of w_e can be made by way of crack opening displacement. If it is assumed, that the load-displacement diagram of a notched specimen is approximately parabolic in shape, the total work of fracture, W_f may be related to the maximum load, P_{max}, and the extension to break, e_b, by the following relationship

$$W_f = \frac{2}{3} P_{max} e_b \tag{10}$$

Using the following relationship for P_{max}

$$P_{max} = mB\sigma_y L \tag{11}$$

and substituting into Equation 10 one obtains;

$$w_f = \frac{2}{3} m\sigma_y e_b \tag{12}$$

which when substituted into Equation 3 gives the following linear relationship between extension to break, e_b, and ligament length, L;

$$e_b = \frac{3}{2m\sigma_y}(w_e + \beta w_p L) \tag{13}$$

The value of e_b at $L = 0$ is identified as the critical crack opening displacement, e_o, from which w_e can be estimated using the following relationship;

$$w_e = \frac{2}{3} m\sigma_y e_o \tag{14}$$

3. Experimental details

3.1. Fracture tests

The effects of specimen width (W), gauge length (Z), geometry, strain rate (v) and temperature (T) on the

TABLE I Experimental programme

Study	Geometry	Specimen size & testing condition
Effect of specimen width (W)	DENT	$Z = 70$ mm, $W = 20$, 35 and 50 mm $v = 5$ mm/min, $T = 23\,^{\circ}$C
Effect of specimen gauge length (Z)	DENT	$W = 35$ mm, $Z = 17$, 35, 70 and 105 mm $v = 5$ mm/min, $T = 23\,^{\circ}$C
Effect of strain rate (v)	DENT	$Z = 70$ mm, $W = 35$ mm $v = 2$, 5, 20 and 50 mm/min, $T = 23\,^{\circ}$C
Effect of test temperature (T)	DENT	$Z = 70$ mm, $W = 35$ mm $v = 5$ mm/min, $T = 23$, 40 and $60\,^{\circ}$C
Effect of specimen geometry	SENT DENT	$Z = 70$ mm, $W = 35$ mm $v = 5$ mm/min, $T = 23\,^{\circ}$C

work of fracture parameters were studied according to the test programme listed in Table I.

To study the effects listed in Table I on the essential and non-essential work of fracture parameters of the uPVC, rectangular coupons of various widths (W) and overall lengths (H) were cut from a rolled uPVC sheet of a nominal thickness 0.26 mm. The length of the coupons was always parallel to the rolling direction of the sheet. The sheet was 500 mm wide and several meters in length. The coupons were then notched to produce series of DENT and SENT specimens with ligament lengths, L, ranging from 2 to 16 mm. A minimum of twenty specimens was tested for the determination of a single w_e value. The measurement of the ligament length was performed prior to testing, using an optical microscope.

After notching, specimens were tested to complete failure in an Instron testing machine using pneumatic clamps. From the recorded load-displacement curves, the following parameters were evaluated and their variations with respect to ligament length, L were studied:

- Net section stress at maximum load, $\sigma_n (= P_{max}/LB)$
- Extension to break, e_b
- Height of the plastic deformation zone, h
- Specific total work of fracture, w_f (total area, W_f, divided by the ligament area $= W_f/LB$)
- Specific work of fracture for yielding, w_y (area up to the maximum load, W_y, divided by the ligament area $= W_y/LB$)
- Specific work of fracture for necking and subsequent tearing, $w_{nt} = w_f - w_y$

3.2. Tensile tests

Determination of the tensile yield stress, σ_y, and Young's modulus, E, as a function of test temperature and the rate of deformation (v) was also carried out using dumbbell-shaped specimens of nominal dimensions $3.8 \times 0.26 \times 75$ mm. Tensile yield stress, σ_y, was calculated using the maximum load and Young's modulus was calculated using the initial slope of the load-displacement curve. Fig. 4 shows some typical tensile load-displacement curves for uPVC at a test speed of 5 mm/min and test temperatures of 23, 40 and 60 °C. These curves show that tensile deformation of uPVC involves necking and cold-drawing. Curves of similar shape were obtained as test speed was changed.

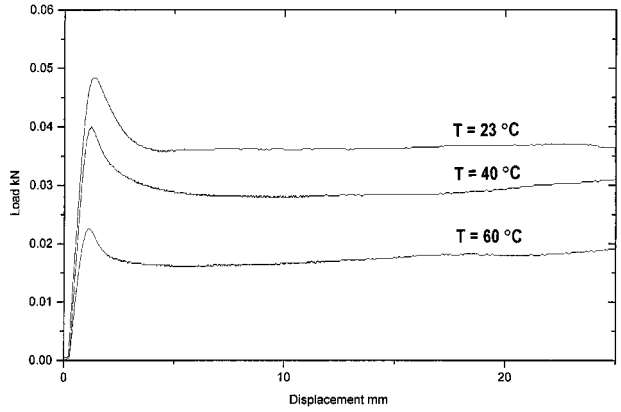

Figure 4 Typical tensile load-displacement diagrams for uPVC.

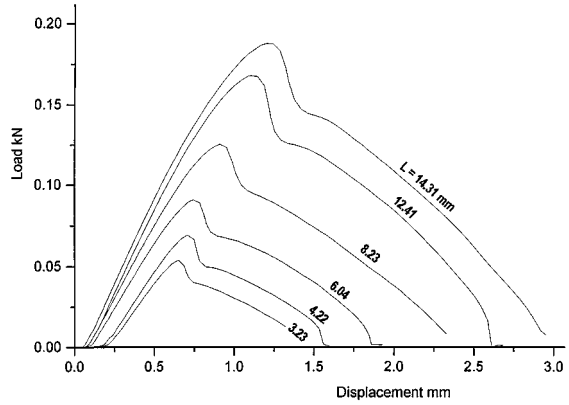

Figure 5 Typical load-displacement diagrams for DENT specimens at room temperature for various ligament lengths, L.

4. Results and discussion

The fracture of all the DENT specimens was completely stable producing load-displacement curves at various ligament lengths of the types shown in Fig. 5.

The visual observation of the DENT specimens during the test, indicated the following sequence of events: opening and blunting of the initial crack tips, formation of a duckbill-shaped yielded zone at each crack tip, complete yielding of the ligament length, ductile tearing of the ligament and finally complete failure of the test specimen. Fig. 6a illustrates the progressive development of a stress-whitened yielded zone at each crack tip in DENT specimens. It was observed that maximum load always corresponded to complete yielding of the ligament area (i.e. when the two yielded zones overlapped mid-way along the ligament length) in DENT

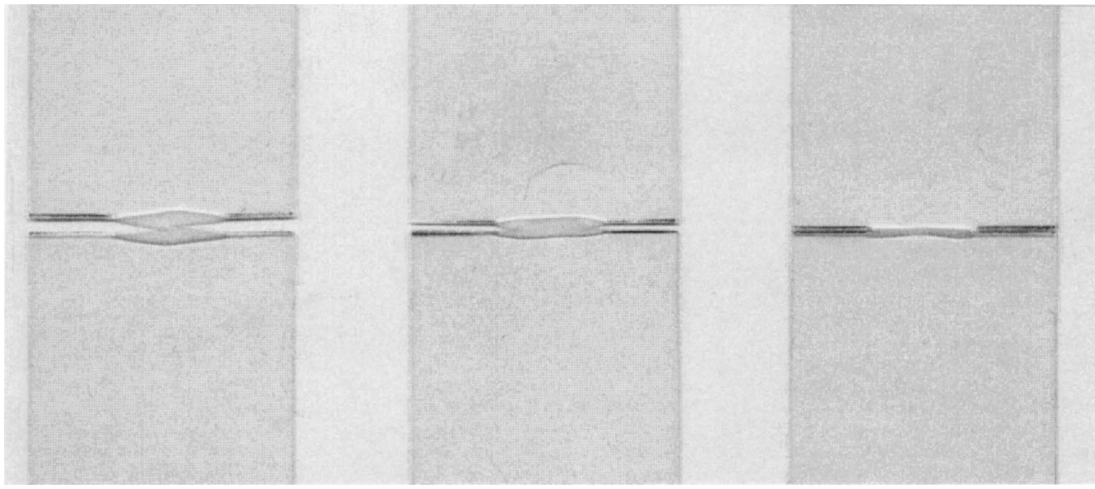

(a)

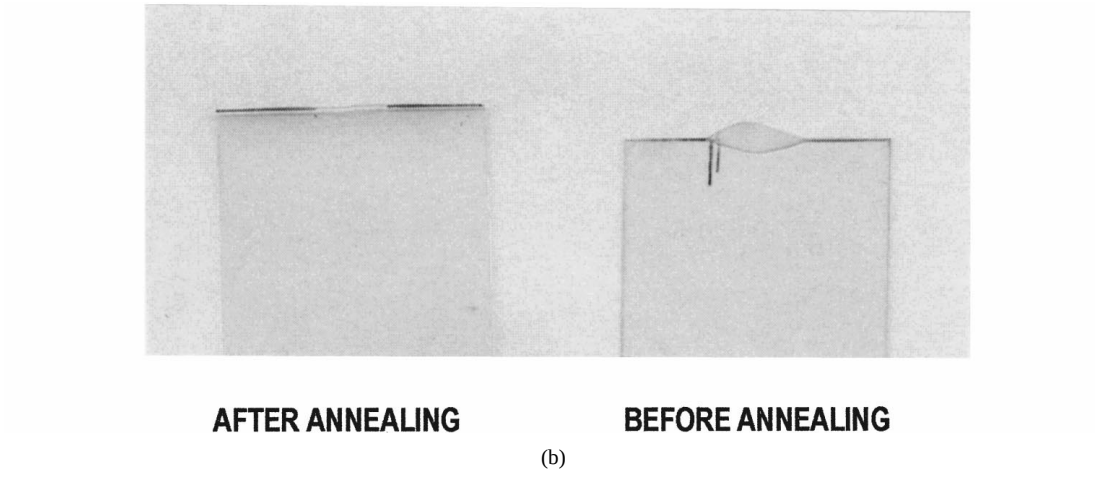

(b)

Figure 6 (a) Progressive development of the inner fracture process zone (IFPZ) and the outer plastic deformation zone (OPDZ) in uPVC at room temperature; (b) Diappearance of the outer plastic deformation zone (OPDZ) in DENT specimens after annealing.

specimens. After yielding, the ligament area necked down giving rise to a sudden load-drop after the maximum load as seen in Fig. 5. This load-drop was sufficient to tear the whole ligament region. It can be said unequivocally, that upon reaching the maximum load, the whole ligament area in DENT specimens yielded instantaneously and therefore the requirement of full ligament yielding was always satisfed.

It was noted, that by keeping the broken specimens for few minutes above the glass transition temperature ($T_g \approx 70\,^{\circ}$C), the plastic deformation zone diminished and the shape of the specimen was full restored ("healed"), as illustrated in Fig. 6b. This healing process which was also observed by Karger-Kocsis et al. [10] in an amorphous copolyester, suggests that no substantial change in the initial entangled network morphology of the polymer structure had taken place due to loading. The recovery of the initial shape of the DENT specimens suggests that cold-drawing, and not, true plastic flow, took place in the plastic zone of this uPVC material.

4.1. Effect of specimen width, *W*

Fig. 7 shows plots of the specific work of fracture parameters, w_f, w_y and w_{nt} versus ligament length, L, for sample widths of 20, 35 and 50 mm. It is seen that for samples widths of 35 and 50 mm, the plots are essentially linear over the whole range of ligament length values used here. As for sample width of 20 mm, a non-linear behaviour was observed in all the plots, as ligament length exceeded 10 mm (i.e. at $L \approx W/2$). The extrapolated values of the specific essential work of fracture parameters w_e, $w_{e,y}$ and $w_{e,nt}$ and their corresponding non-essential work parameters (βw_p, $\beta_y w_{p,y}$ and $\beta_{nt} w_{p,nt}$), for different specimen widths were determined from the linear regression lines drawn in Fig. 7. The extrapolated values and slopes are given in Table II with their 95% confidence limits.

TABLE II Effect of specimen width, W, on the specific work of fracture parameters ($v = 5$ mm/min, $Z = 70$ mm, $T = 23\,^{\circ}$C)

Fracture parameters	$W = 20$ mm	$W = 35$ mm	$W = 50$ mm
w_e (kJ/m^2)	34.69 ± 2.54	35.02 ± 2.60	34.43 ± 1.46
$w_{e,y}$ (kJ/m^2)	13.01 ± 2.21	11.90 ± 1.36	12.53 ± 0.67
$w_{e,nt}$ (kJ/m^2)	21.68 ± 1.90	22.64 ± 2.16	21.56 ± 1.46
βw_p (MJ/m^3)	2.80 ± 0.27	3.27 ± 0.28	3.00 ± 0.16
$\beta_y w_{p,y}$ (MJ/m^3)	2.11 ± 0.16	1.62 ± 0.15	1.27 ± 0.07
$\beta_{nt} w_{p,nt}$ (MJ/m^3)	0.87 ± 0.19	1.68 ± 0.23	1.73 ± 0.15

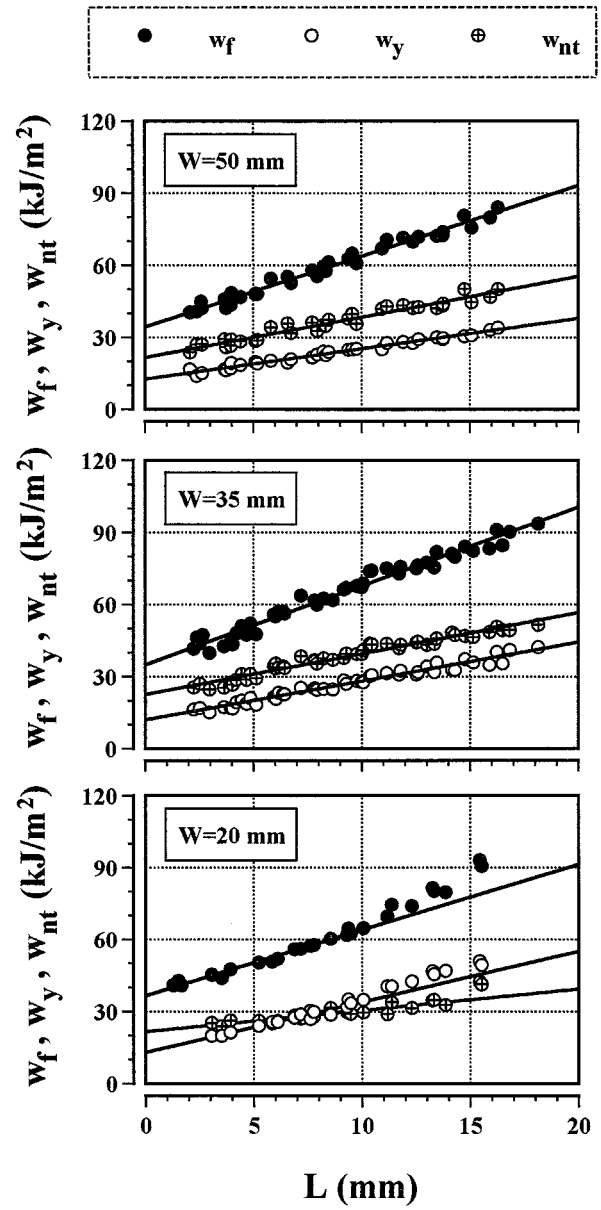

Figure 7 Specific work of fracture parameters versus ligament length, L, for specimen widths, W, of 50, 35 and 20 mm; $T = 23\,^{\circ}$C, $Z = 70$ mm and $v = 5$ mm/min.

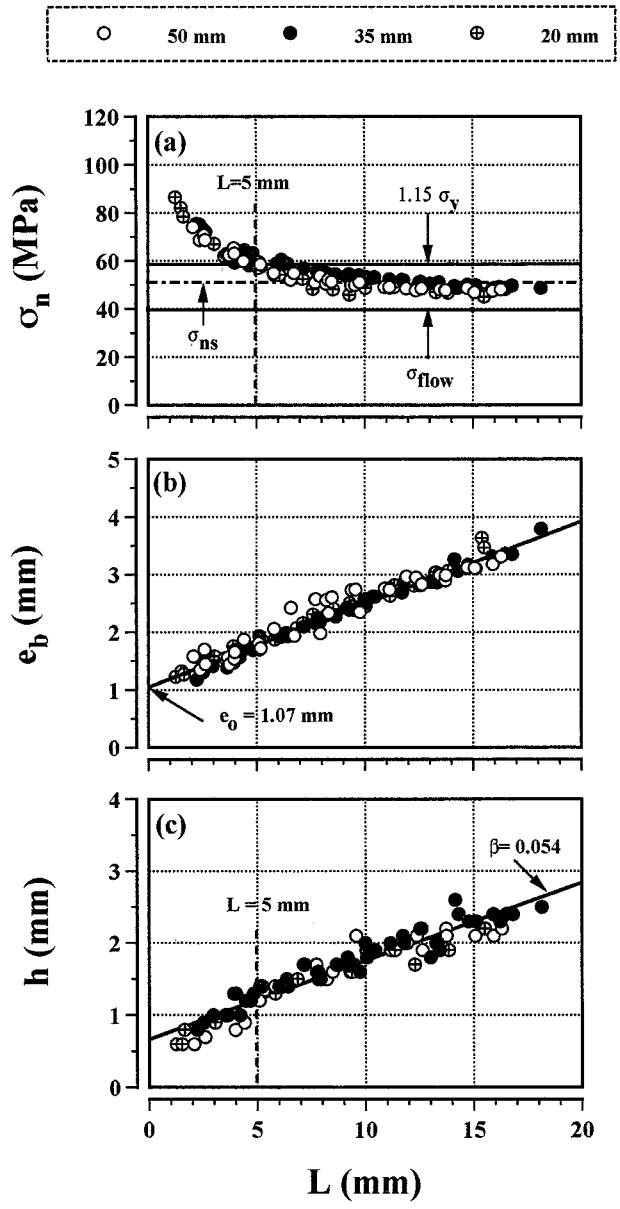

Figure 8 Net-section stress, σ_n, extension to break, e_b, and the height of the plastic zone, h, versus ligament length for specimen widths, W, of 50, 35 and 20 mm; $T = 23\,^{\circ}$C, $Z = 70$ mm and $v = 5$ mm/min.

It may be deduced, that the essential work terms are independent of specimen width. The fact that these energy terms are unaffected by W indirectly confirms that plane stress conditions are achieved in the ligament region. It is also evident that almost 63% of w_e is contributed by the necking/tearing process, i.e. $w_{e,nt}$.

As for non-essential work terms, it is seen that whilst βw_p is more or less independent of W, $\beta_y w_{p,y}$ and $\beta_{nt} w_{p,nt}$ values are strongly dependent upon W; the latter increasing and the former decreasing with increasing W.

The dependence of the net-section stress at the maximum load (σ_n), extension to break (e_b) and the height of the plastic deformation zone (h) on ligament length for specimen widths of 20, 35 and 50 mm are shown in Fig. 8.

It is seen from Fig. 8a, that σ_n is more or less independent of W, but very much dependent on the ligament length, L. As stated earlier, owing to plastic constraint imposed by the notches, the net-section stress for DENT geometry is expected to rise to 1.15 times the uniaxial yield stress of the material (σ_y). However, it is evident from Fig. 8a, that σ_n decreases steadily with increasing L, reaching a steady state value (σ_{ns}), at large ligament lengths. According to Fig. 8a, $\sigma_{ns} \approx \sigma_y$ and not the theoretical value of $1.15\sigma_y$. Moreover, as clearly illustrated in Fig. 4, while at 23 °C, the material yields at 51 MPa, due to strain-softening, it undergoes cold drawing at a constant stress value of approximately $0.78\sigma_y$ (i.e. $\sigma_{flow} \approx 40$ MPa). It may be reasonable to assume, that within the plastic deformation zone, the stress is approximately $1/2(\sigma_y + \sigma_{flow}) = \sigma_u$. If this approximation is accepted, then for large ligament lengths we have, $\sigma_{ns} \approx 1.15\sigma_u$. However, one only needs to refer to studies by Wu & Mai on linear low density polyethylene [12], Karger-Kocsis et al. on an amorphous copolyester [9, 10] and Hashemi on a wide range of polymeric films [5, 8], to realize that the requirement that $\sigma_{ns} = 1.15\sigma_y$ is very rarely achieved in polymers that show strain softening phenomenon. What stems from these studies

is that the linearity between w_f and L is preserved as long as σ_n attains some steady state value. The stress ratio σ_{ns}/σ_y appears to be dependent upon the degree of strain softening experienced by the material as well as the geometry of the notched specimen.

As for the requirement that L should be less than $W/3$ to avoid disturbance of the plastic zone by the edge effects, it is seen from the data presented here, that this condition is too restrictive. The experimental data for $W = 20$ mm, suggests a more conservative requirement of $L \leq W/2$, for eliminating edge effects.

The requirements that L should be less than $2R_p$, is also found to be too restrictive. By substituting values of $w_e \approx 34.62$ kJ/m^2, $E = 3.36$ GPa and $\sigma_y = 51$ MPa into Equation 6 we obtain that $2R_p \approx 14$ mm. However, when considering, that ligament region of all DENT specimens was yielded fully, as indicated by the sudden load-drop, this condition appears also to be too restrictive for uPVC. Consequently, neither of the two requirements give an accurate estimation of the upper limit value of the ligament length. Indeed, previous studies [e.g. 5, 8, 9, 10] led to the same conclusion regarding both of the aforementioned requirements.

Another feature of Fig. 8a which is worthy of consideration, is the elevated values of σ_n at small ligament lengths. This behaviour is often attributed to the change in the stress state in the ligament region. According to Equation 5, a transition from a pure plane-stress fracture to a mixed mode fracture is expected at a ligament length value of about $3B$–$5B$. This corresponds to a ligament length value in the region of 0.8 to 1.8 mm in this study for which B is 0.26 mm. However, according to Fig. 8a, plane-stress/plane-strain transition in uPVC occurs at a ligament length value in the region of 3.5–5 mm, i.e. L/B ratio of 13–19. Several studies using different types of polymeric films have also indicated a large L/B ratio at the transition point. For example, Wu & Mai [12] noted that for LLDPE film the plane-strain/plane-stress transition occurs at $L/B = 14$, Hashemi [5] observed that for PBT/PC blend the transition occurs at $L/B = 20$ while Li et al. [16] did not observe any transition for PP/elastomer blend nor did Karger-Kocsis et al. [9, 10] in their study on amorphous copolyester film of thickness of 0.5 mm. These finding raise the question as to whether the proposed requirement that L/B ratio should exceed 3–5 is indeed universal or that the ratio depends on the type of material that is used.

As the plane-strain value of the specific work of fracture is lower than the plane-stress value, it is expected that in the mixed mode region, w_f values fall below the linear regression line that describes the variation of w_f with L in the region of pure plane-stress. Surprisingly, there is no strong evidence of such nonlinearity at small ligament lengths (i.e. $L < 3.5$–5 mm) in any of the plots presented Fig. 7. Indeed, exclusion of the data for which ligament length had values of less than 3.5–5 mm, only marginally altered the values of the specific essential and non-essential work of fracture parameters given in Table II; the values were well within the ±95% confidence limits.

As regards the dependence of the extension to break (e_b) on ligament length, it is evident from Fig. 8b that not only the dependence is very linear as suggested by Equation 13, it is also independent of the specimen width. The linear extrapolation of the data to $L = 0$ gives a crack opening displacement (e_0) value of 1.07 mm. To estimate w_e via Equation 14, an appropriate choice of value for the quantity $m\sigma_y$ is required. It is the author's opinion, that the quantity $m\sigma_y$ should be replaced by the steady state value of the net-section stress (σ_{ns}) which according to Fig. 8a has a value close to σ_y (or alternatively as $1.15\sigma_u$). This gives a w_e value of 36.4 kJ/m^2, which agrees quite well, with the average value of 34.62 kJ/m^2 obtained directly from the plots of w_f vs L.

According to Equation 4, the overall height of the plastic zone, h, is a linear function of the ligament length, L. This relationship is corroborated by the experimental results presented in Fig. 8c. The variation appears to be insensitive to W. The best linear regression line through the data in Fig. 8c, gives a plastic zone shape factor (β) of 0.054. Given that $\beta w_p \approx 3.14$ MJ/m^2, we estimate a specific plastic work (w_p) value of 58 MJ/m^2, for this uPVC sheet.

4.2. Effect of Specimen Gauge Length, Z

The load-displacement curves for all values of Z used here, were similar to those presented in Fig. 5, i.e. mode of failure was not affected by Z.

Fig. 9 shows plots of the specific work of fracture parameters, w_f, w_y and w_{nt} vs. ligament length, L, for specimen gauge lengths (Z) of 17, 35 and 105 mm (plots for the gauge length of 70 mm can be found in Fig. 7). It is seen that plots are essentially linear over the whole ligament range. As demonstrated, change in Z affects values of w_y and w_{nt} in a different way. It is observed that whereas w_{nt} decreases, w_y increases, with increasing Z. As shown in Fig. 9, the greater contribution to w_f for Z values of 17, 35 and 70 mm, stems from the necking/tearing component (w_{nt}). For the gauge length of 105 mm, the yielding contribution is close to, and for large ligament lengths even exceeds the necking/tearing contribution. This suggests, that larger values of Z could lead to instability of the DENT test specimens. Results further demonstrate that requirements that $L < 2R_p$ and $L < W/3$ are once again too stringent for uPVC material.

The extrapolated values of the specific essential work of fracture parameters w_e, $w_{e,y}$ and $w_{e,nt}$ and their corresponding non-essential work parameters (βw_e, $\beta_y w_{e,y}$ and $\beta_{nt} w_{e,nt}$), for different gauge lengths were determined from the linear regression lines drawn in Fig. 9. The extrapolated values and slopes are given in Table III with their 95% confidence limits.

It can be observed, that change in gauge length has no significant effect upon the measured values of the specific essential work of fracture parameters. This confirms, once more, that the state of stress in the ligament region is that of pure plane stress. Almost 63% of the total specific essential work of fracture (w_e) stems from the necking/tearing component, $w_{e,nt}$.

It is worth stating at this stage, that values of the specific essential work terms (w_e, $w_{e,y}$, $w_{e,nt}$) are

TABLE III Effect of specimen gauge length, Z, on the specific work of fracture parameters ($v = 5$ mm/min, $W = 35$ mm, $T = 23\,^{\circ}$C)

Fracture parameter	$Z = 17$ mm	$Z = 35$ mm	$Z = 70$ mm	$Z = 105$ mm
w_e (kJ/m^2)	35.10 ± 1.57	33.73 ± 1.73	35.02 ± 2.60	32.64 ± 1.54
$w_{e,y}$ (kJ/m^2)	10.27 ± 1.17	10.98 ± 0.75	11.90 ± 1.36	10.58 ± 1.23
$w_{e,n}$ (kJ/m^2)	24.84 ± 1.80	22.75 ± 1.38	22.64 ± 2.16	22.07 ± 1.21
βw_p (MJ/m^3)	3.40 ± 0.16	3.00 ± 0.15	3.27 ± 0.28	3.75 ± 0.16
$\beta_y w_{p,y}$ (MJ/m^3)	0.72 ± 0.13	1.11 ± 0.06	1.62 ± 0.15	2.46 ± 0.12
$\beta_{nt} w_{p,nt}$ (MJ/m^3)	2.68 ± 0.20	1.89 ± 0.12	1.68 ± 0.23	1.30 ± 0.12

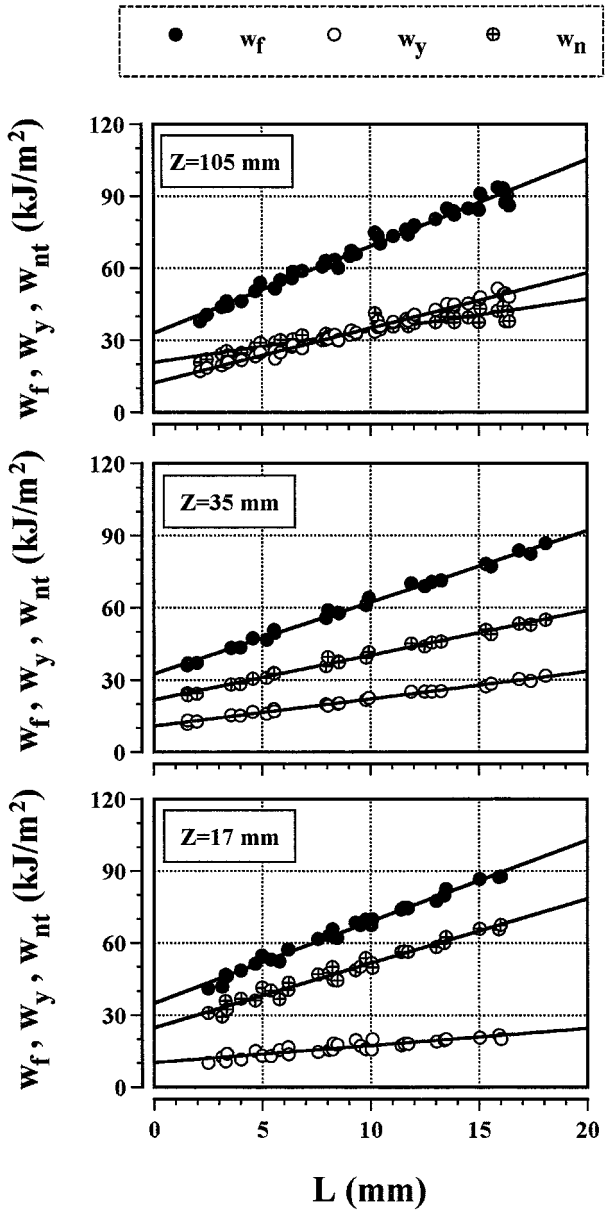

Figure 9 Specific work of fracture parameters versus ligament length, L, for gauge length values, Z, values of 105, 35 and 17 mm; $T = 23\,^{\circ}$C, $W = 35$ mm and $v = 5$ mm/min.

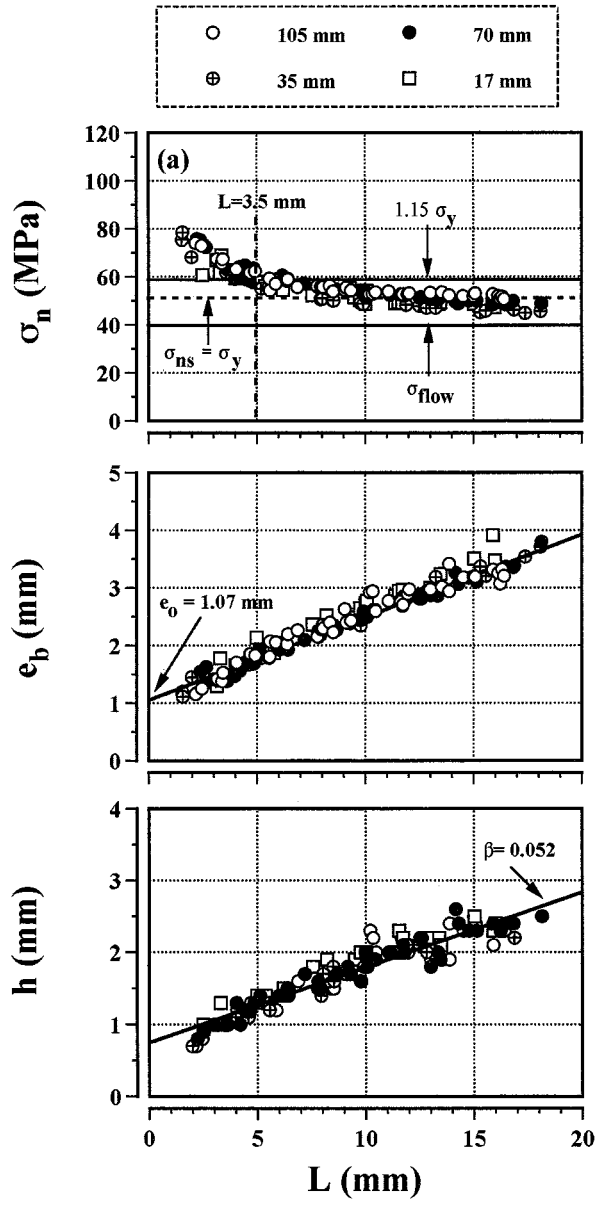

Figure 10 Net-section stress, σ_n, extension to break, e_b, and the height of the plastic zone, h, versus ligament length for specimen gauge lengths, Z, of 105, 70, 35 and 17 mm; $T = 23\,^{\circ}$C, $W = 35$ mm and $v = 5$ mm/min.

practically independent of both Z and W. This confirms that the specific essential work terms are indeed "material constants" for a given thickness.

As for non-essential work terms, it is observed that whereas βw_p is not significantly influenced by Z, $\beta_y w_{p,y}$ and $\beta_{nt} w_{p,nt}$ values are affected significantly by Z; the latter decreasing and the former increasing with increasing Z. The combined effect of specimen width and gauge length on $\beta_y w_{p,y}$ and $\beta_{nt} w_{p,nt}$ values is illustrated in Fig. 10, where values are plotted against the ratio Z/W. It is seen that $\beta_y w_{p,y}$ decreases and $\beta_{nt} w_{p,nt}$ increases, with increasing Z/W. The two curves intersect at a Z/W ratio of approximately 2. At this ratio, $\beta_y w_{p,y} \approx \beta_{nt} w_{p,nt} \approx 1/2 \beta w_p$.

The plots of net-section stress at maximum load, σ_n, extension to break, e_b, and the height of the plastic zone, h, vs. ligament length are shown in Fig. 11. It is observed, that these plots follow the same trend as

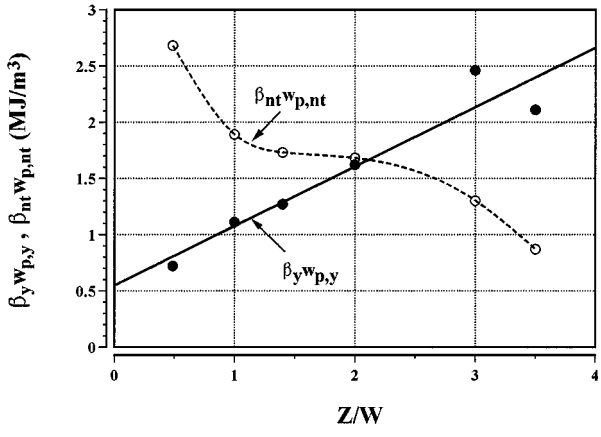

Figure 11 Effect of Z/W ratio on non-essential work of fracture parameters for yielding and necking/tearing.

when W was changed (see Fig. 9). Indeed as depicted in Figs 10b and 10c, values of e_o and β do not differ significantly from those of Figs 8a and 8b. It may be inferred, that these parameters are also independent of both W and Z, for a given thickness.

4.3. Effect of loading rate

All the DENT specimens tested at the loading rates (v) of 2, 5, 20 and 50 mm/min failed in a ductile manner. The load-displacement curves obtained from these tests were similar to those presented in Fig. 5. The tensile load-displacement curves obtained from dumbbell-shaped specimens also exhibited ductile failure (necking and cold-drawing as in Fig. 4) at these loading rate values. The tensile yield stress at maximum load (σ_y) and elastic modulus (E) evaluated from these curves can be found in Table IV ($\pm$ represents standard deviation about the mean value). It is seen that the yield stress and modulus both increase with increasing rate. The ratio of flow stress to tensile yield stress (i.e. σ_{flow}/σ_y) was rate insensitive and was consistently around 0.78 ± 0.02.

Fig. 12 shows plots of the specific work of fracture terms vs. ligament length for loading rate values of 2, 20 and 50 mm/min (plots for loading rate of 5 mm/min can be found in Fig. 7). The extrapolated values of the specific essential work of fracture parameters and their corresponding non-essential work parameters were determined from the linear regression lines drawn in Fig. 12. The extrapolated values and slopes with their 95% confidence limits are given in Table IV. It can be observed, that for the range of loading rate values used

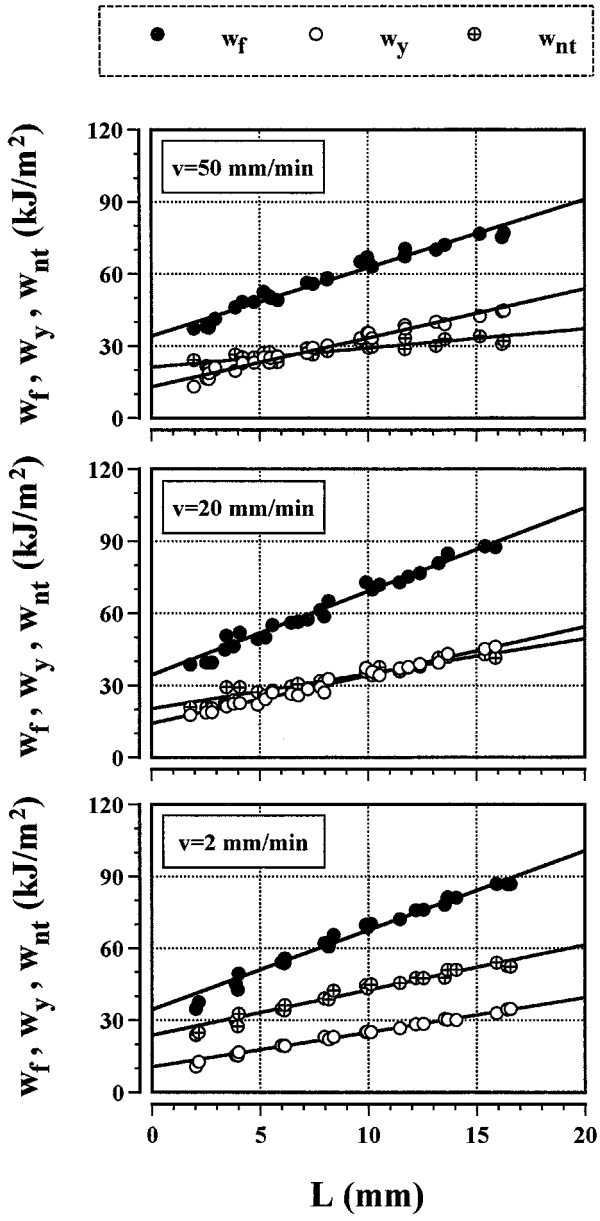

Figure 12 Specific work of fracture parameters versus ligament length, L, at deformation rates, v, of 50, 20 and 2 mm/min; $T = 23\,^{\circ}$C, $W = 35$ mm and $Z = 70$ mm.

here, w_e is indeed rate insensitive, as are $w_{e,y}$ and $w_{e,nt}$ values.

The specific non-essential work terms show some variation with respect to v. One may observe that whereas $\beta_y w_{p,y}$ increases, $\beta_{nt} w_{p,nt}$ decreases with increasing rate. It is seen also, that although at lower rates of 2 and 5 mm/min, the specific work of fracture for

TABLE IV Effect of loading rate, v (mm/min), on the specific work of fracture parameters ($Z = 70$ mm, $W = 35$ mm, $T = 23\,^{\circ}$C)

Fracture parameter	$v = 2$	$v = 5$	$v = 20$	$v = 50$
σ_y (MPa)	49.74 ± 1.17	51.00 ± 209	54.03 ± 1.16	57.69 ± 1.32
E (GPa)	3.25 ± 0.21	3.36 ± 0.11	3.45 ± 0.08	3.51 ± 0.09
w_e (kJ/m^2)	34.49 ± 2.01	35.02 ± 2.60	34.39 ± 2.40	34.20 ± 2.06
$w_{e,y}$ (kJ/m^2)	11.00 ± 0.51	11.90 ± 1.36	13.39 ± 1.20	13.04 ± 1.29
$w_{e,nt}$ (kJ/m^2)	23.49 ± 1.87	22.64 ± 2.16	21.00 ± 1.13	21.16 ± 1.62
βw_p (MJ/m^3)	3.32 ± 0.20	3.27 ± 0.28	3.47 ± 0.15	2.84 ± 0.23
$\beta_y w_{p,y}$ (MJ/m^3)	1.45 ± 0.06	1.62 ± 0.15	2.02 ± 0.14	2.04 ± 0.14
$\beta_{nt} w_{p,nt}$ (MJ/m^3)	1.87 ± 0.18	1.68 ± 0.23	1.46 ± 0.11	0.80 ± 0.17
$2R_p$ (mm)	14.42	14.40	12.94	11.48

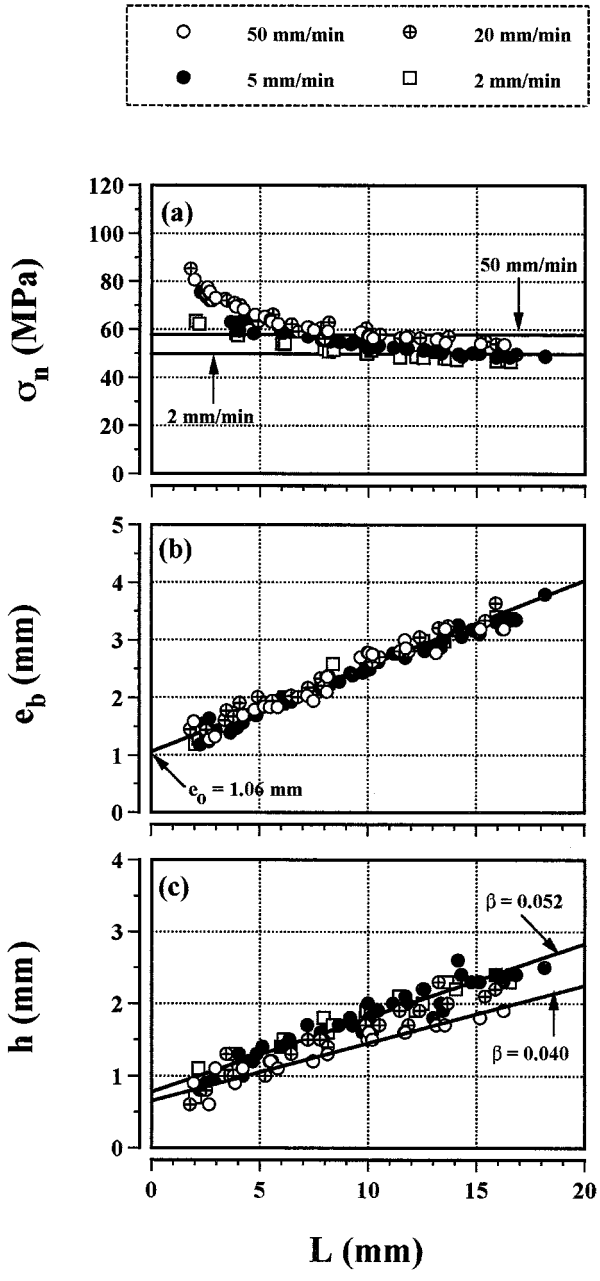

Figure 13 Plots of net-section stress, σ_n, extension to break, e_b, and the height of the plastic zone, h, versus ligament length, L, at deformation rates, v, of 50, 20, 5 and 2 mm/min; $T = 23\,^{\circ}$C, $W = 35$ mm and $Z = 70$ mm.

yielding, $w_{p,y}$ is significantly lower than that of necking/tearing, at higher rates (e.g. 20 and 50 mm/min), it is close and even exceeds necking/tearing contribution ($w_{p,nt}$).

The effect of loading rate on net-section stress, extension to break and the overall height of the plastic zone can be found in Fig. 13. Generally speaking, variation for each parameter with respect to ligament length is similar to what has been found thus far, in this study. It is seen from Fig. 13a that $\sigma_{ns} \approx \sigma_y$ at each rate. Of particular interest are the plots of e_b and h as shown in Figs 13b and 13c, respectively. Fig. 13b shows that extension to break is independent of loading rate. The extrapolated value, e_o, agrees quite well with values determined from the width and gauge length studies. This further supports the view that direct and indirect measurements of w_e are in good agreement.

Figure 13c shows that the overall height of the plastic zone may depend on the loading rate. The best linear regression lines drawn through the 2 mm/min and 50 mm/min, gave β values of 0.040 and 0.052 respectively. The data however, contains high degree of scatter which prevent us to say, with some degree of certainty, as to whether h is dependent on or indeed independent of, the loading rate.

4.4. Effect of temperature

Figs 14a and 15a show typical load-displacement curves for DENT specimens with various ligament lengths at test temperatures of 40 °C and 60 °C respectively. The curves show the same features as the load-displacement curves at room temperature (see Fig. 5). The main differences being, lower maximum load and greater extension to break, as temperature is increased. As illustrated in Figs 14b and 15b, the sequence of events happening during crack propagation also follows that of the room temperature tests. The main differences being, a greater crack opening displacement and volume of plastic deformation zone at higher temperatures, for the same ligament length value.

The effects of temperature on the specific work of fracture terms, net-section stress at maximum load, extension to break and the height of the plastic deformation zone are shown in Figs 16 and 17 for test temperatures of 40 °C and 60 °C respectively.

Figs 16a and 17b show the variation of specific work of fracture terms as a function of the ligament length. It is seen that increase in temperature reduces w_y but increases w_{nt}. This is expected as values of tensile yield stress and extension to yield, both decreased with increasing temperature. As a consequence, less energy is required for the material in the ligament region to yield. On the other hand, increase in temperature leads to a larger crack opening displacement which in turn increases the energy required for tearing of the ligament region. Table V compares the values of the specific essential and non-essential work terms for the three test temperatures. Also given in Table V are the values of tensile yield stress and modulus at each test temperature. It is evident, that whereas w_e is practically insensitive to temperature, $w_{e,y}$ and $w_{e,nt}$ are both affected strongly by the temperature. The latter increasing and the former decreasing with increasing temperature for reasons already discussed. As for the non-essential

TABLE V Fracture parameters as a function of test temperature, T ($v = 5$ mm/min, $W = 70$ mm, $Z = 70$ mm)

Fracture parameter	$T = 23\,^{\circ}$C	$T = 40\,^{\circ}$C	$T = 60\,^{\circ}$C
σ_y (MPa)	51.00 ± 209	41.50 ± 0.94	25.00 ± 1.89
E (MPa)	3.36 ± 0.11	3.19 ± 0.11	2.16 ± 0.074
w_e (kJ/m^2)	35.02 ± 2.60	35.18 ± 1.99	34.50 ± 2.02
$w_{e,y}$ (kJ/m^2)	11.90 ± 1.36	8.40 ± 0.89	5.92 ± 0.50
$w_{e,nt}$ (kJ/m^2)	22.64 ± 2.16	26.78 ± 2.19	28.65 ± 2.24
βw_p (MJ/m^3)	3.27 ± 0.28	3.82 ± 0.19	4.43 ± 0.22
$\beta_y w_{p,y}$ (MJ/m^3)	1.62 ± 0.15	1.17 ± 0.09	0.73 ± 0.05
$\beta_{nt} w_{p,nt}$ (MJ/m^3)	1.68 ± 0.23	2.65 ± 0.20	3.70 ± 0.24
w_p (MJ/m^3)	62.89	51.37	32.82
$2R_p$ (mm)	14.40	21.21	37.95

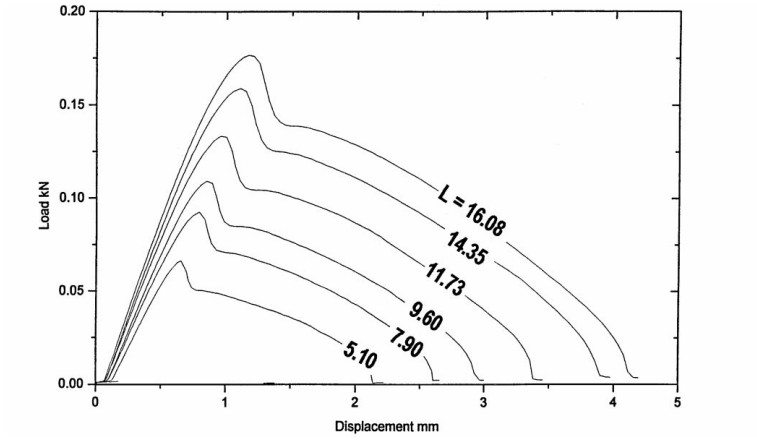

(a)

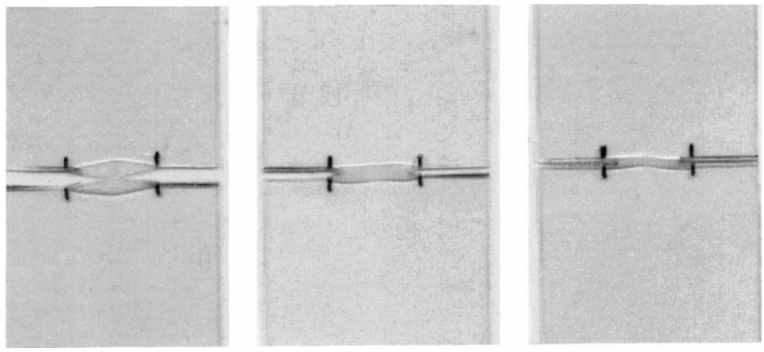

(b)

Figure 14 (a) Typical load-displacement diagrams for DENT specimens at 40 °C for various ligament lengths, *L*; (b) Progressive development of the inner fracture process zone (IFPZ) and the outer plastic deformation zone (OPDZ) in uPVC at 40 °C.

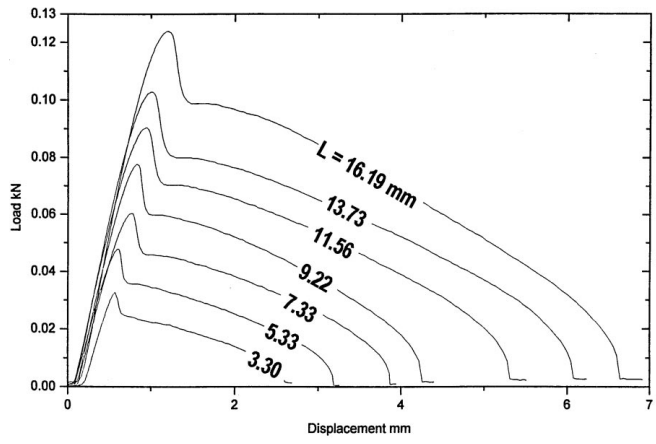

(a)

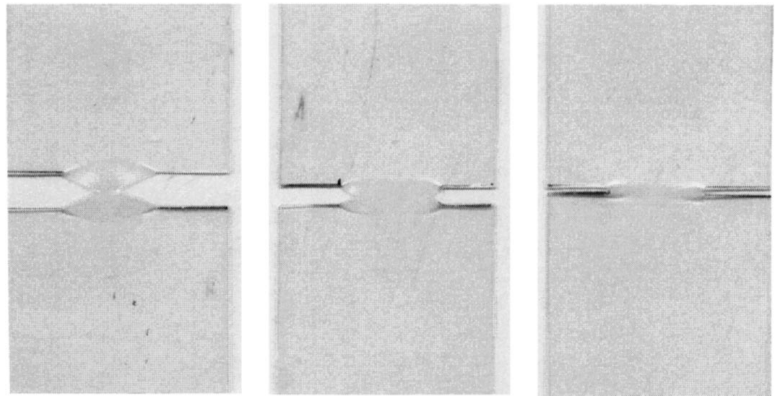

(b)

Figure 15 (a) Typical load-displacement diagrams for DENT specimens at 60 °C for various ligament lengths, *L*; (b) Progressive development of the inner fracture process zone (IFPZ) and the outer plastic deformation zone (OPDZ) in uPVC at 60 °C.

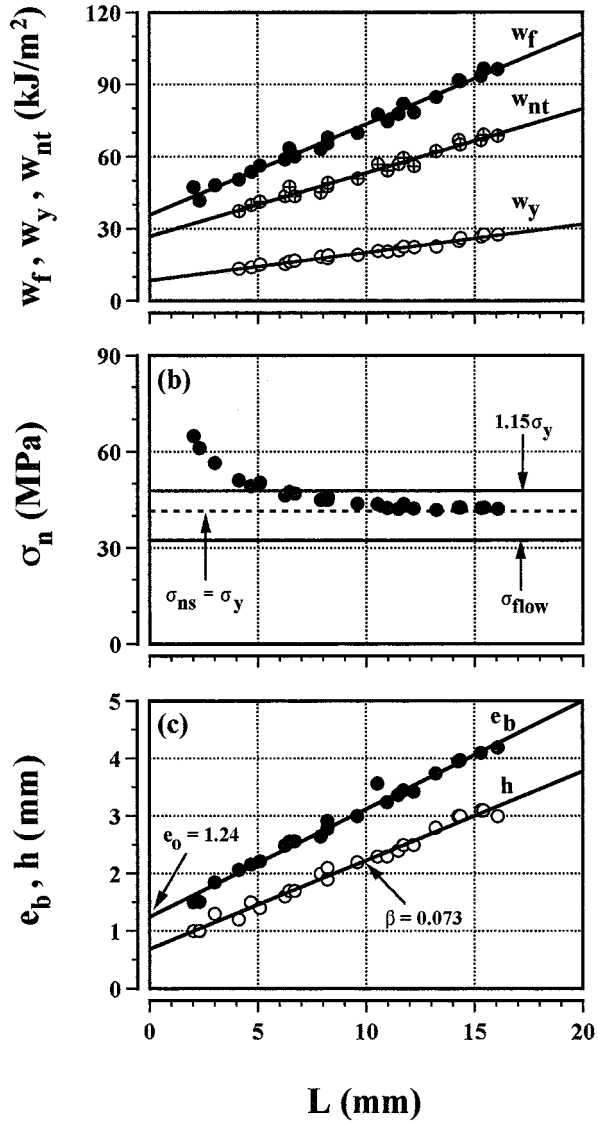

Figure 16 Plots of the specific work of fracture parameters, net-section stress, σ_n, extension to break, e_b, and the height of the plastic zone, h, versus ligament length, L, at 40 °C; $W = 35$ mm, $Z = 70$ mm and $v = 5$ mm/min.

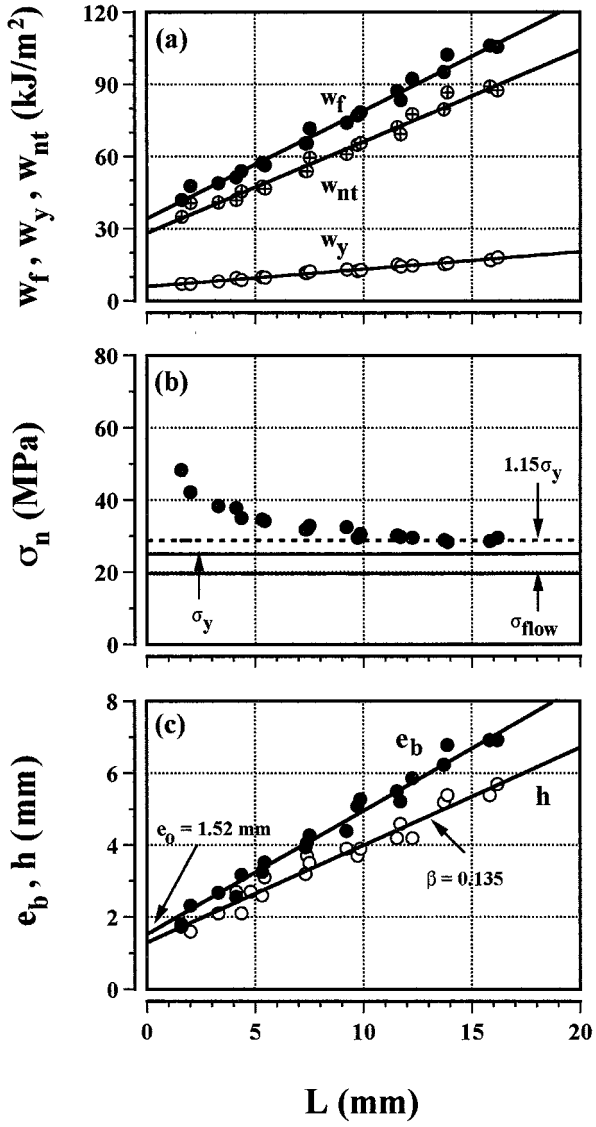

Figure 17 Plots of the specific work of fracture parameters, net-section stress, σ_n, extension to break, e_b, and the height of the plastic zone, h, versus ligament length, L, at 60 °C; $W = 35$ mm, $Z = 70$ mm and $v = 5$ mm/min.

work terms, it is observed that whilst βw_p and $\beta_{nt} w_{p,nt}$ increase with increasing temperature, $\beta_y w_{p,y}$ decreases with increasing temperature.

As for the effect of temperature on net-section stress, it is observed from Figs 16b and 17b, that the steady state value, σ_{ns}, reaches $1.15\sigma_y$ as temperature is increased. This suggests, that σ_{ns} depends not only on the material, but also on the conditions to which it is subjected to. The universal condition that $1.15\sigma_y$ therefore needs to be carefully studied.

As for the effect of temperature on extension to break, it can be deduced from Figs 16b and 16c and also 8c that extension to break increases with increasing temperature. Moreover, as depicted in these figures, the crack opening displacement value, e_o, also increases with increasing temperature. This is consistent with the photographs shown in Figs 6a, 14b and 15b. Using the proposed relationship that $w_e = 2/3 e_o \sigma_{ns}$, we estimate w_e values of 34.31 kJ/m^2 and 30 kJ/m^2 for 40 °C and 60 °C respectively. These values further confirm that w_e is not very sensitive to changes in temperature.

As far as the shape factor, β, is concerned, it is seen that β increases from a value of 0.052 at 23 °C to a value of 0.135 at 60 °C. As shown in Table V, the estimated value of plastic work done, w_p, decreases with increasing temperature.

4.5. Effect of specimen geometry

To study the effect of specimen geometry on fracture parameters, several SENT specimens of dimensions $W = 35$ mm, $Z = 70$ mm were prepared from the same uPVC roll and tested at room temperature at a constant loading rate of 5 mm/min. Fig. 18a shows typical load-displacement curves obtained for SENT specimen at various ligament lengths. These curves indicate that SENT specimens like DENT fail by ductile tearing of the ligament region. However, there was no evidence of load-drop at maximum load in any of the SENT curves obtained in this study. It is worth pointing out that firstly, the full yielding of the ligament region in SENT specimens occurred only when $L \leq 7$ mm. This is illustrated by the photographs in Fig. 18b, where each specimen

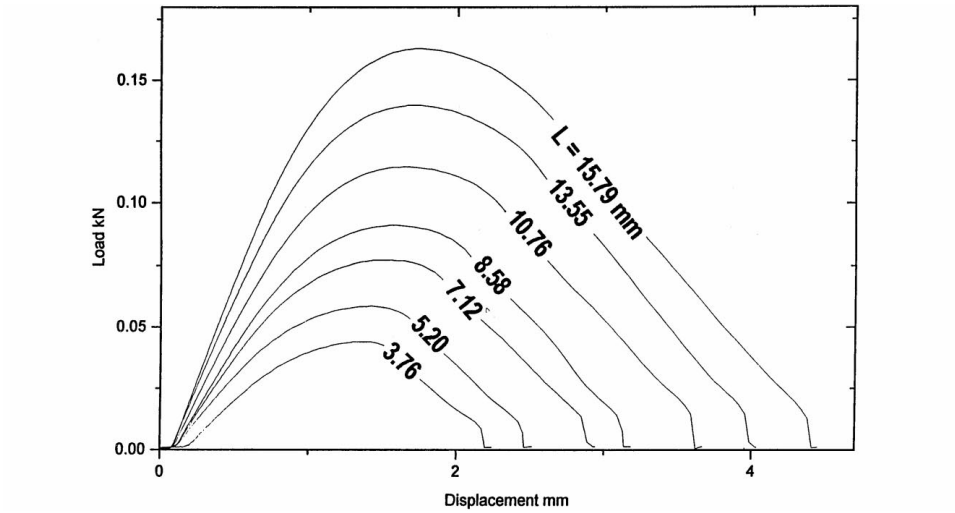

(a)

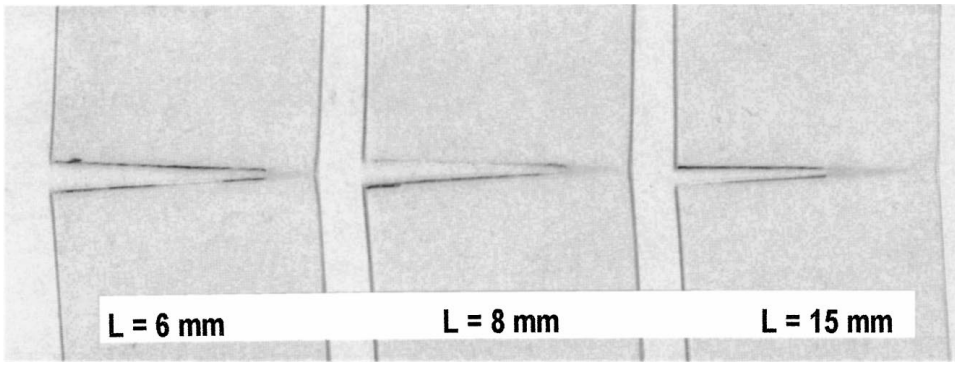

(b)

Figure 18 Typical load-displacement diagrams for SENT specimens at 23 °C for various ligament lengths, L; (b) The extent of the outer plastic deformation zone (OPDZ) at maximum load in SENT specimens with different ligament lengths.

in the photograph was unloaded as maximum load was reached. Secondly, crack growth in SENT specimens was initiated prior to attainment of maximum load.

Fig. 19a compares the plot of σ_n versus ligament length for both geometries. It is seen that σ_n for SENT specimens is always lower than that of DENT specimens. Whilst for DENT geometry, $\sigma_{ns} \approx \sigma_y$, for SENT geometry we have $\sigma_{ns} \approx 0.78\sigma_y$ or $\sigma_{ns} \approx \sigma_{flow}$. The steady state value (σ_{ns}) appears to have been reached once the ligament length exceeded 5 mm. As illustrated in Fig. 19b, plots of the specific work of fracture terms were linear over the whole range of ligament length values. This may be attributed to the localised nature of the duckbill-shaped plastic zone at the tip of the crack.

The comparison of Fig. 19b with Fig. 7b clearly demonstrates that for the specimen dimensions and testing conditions, the relative position of the plots of w_y and w_{nt} vs. ligament length is different for two geometries. Whereas in DENT specimens, w_{nt} was always greater that w_y for all values of L, in SENT specimens $w_{nt} > w_y$ for $L < 7$ mm and $w_{nt} < w_y$ for $L > 7$ mm. It must be noted however, that only for ligament length values of 7 mm and less, the complete yielding of the ligament region, coincided with maximum load. Consequently the way in which w_y and w_{nt} values are calculated is not strictly accurate for $L > 7$ mm. The extrapolated values w_e, $w_{e,y}$ and $w_{e,nt}$ are nonetheless given in Table VI and compared with the values obtained by

TABLE VI Fracture parameters for SENT and DENT specimens ($v = 5$ mm/min, $W = 70$ mm, $Z = 70$ mm)

Fracture parameter	DENT	SENT
w_e (kJ/m^2)	35.02 ± 2.60	43.48 ± 2.75
$w_{e,y}$ (kJ/m^2)	11.90 ± 1.36	12.47 ± 3.87
$w_{e,nt}$ (kJ/m^2)	22.64 ± 2.16	30.91 ± 1.60
βw_p (MJ/m^3)	3.27 ± 0.28	4.62 ± 0.31
$\beta_y w_{p,y}$ (MJ/m^3)	1.62 ± 0.15	3.76 ± 0.27
$\beta_n w_{p,nt}$ (MJ/m^3)	1.68 ± 0.23	0.87 ± 0.18
e_b (mm)	1.07 ± 0.07	1.47 ± 0.12

way of DENT specimens. It is seen that as far as the specific essential work terms are concerned, values of w_e and $w_{e,nt}$ for SENT are higher than the corresponding values for DENT. However, both geometries give a similar $w_{e,y}$ value. It may be suggested that $w_{e,y}$ may represent the initiation value of the specific essential work of fracture in uPVC.

It can be observed also that the specific non-essential work of fracture, βw_p, for SENT specimens is higher than that of DENT specimens. This difference is commonly attributed to the difference in the plastic zone shape factor, β, of the two geometries. It is seen from Fig. 19c that a linear relationship exist between the height of the plastic zone in SENT specimens and the ligament length. From the slope of the line which is 2β, we obtain a β value 0.143 for SENT specimens

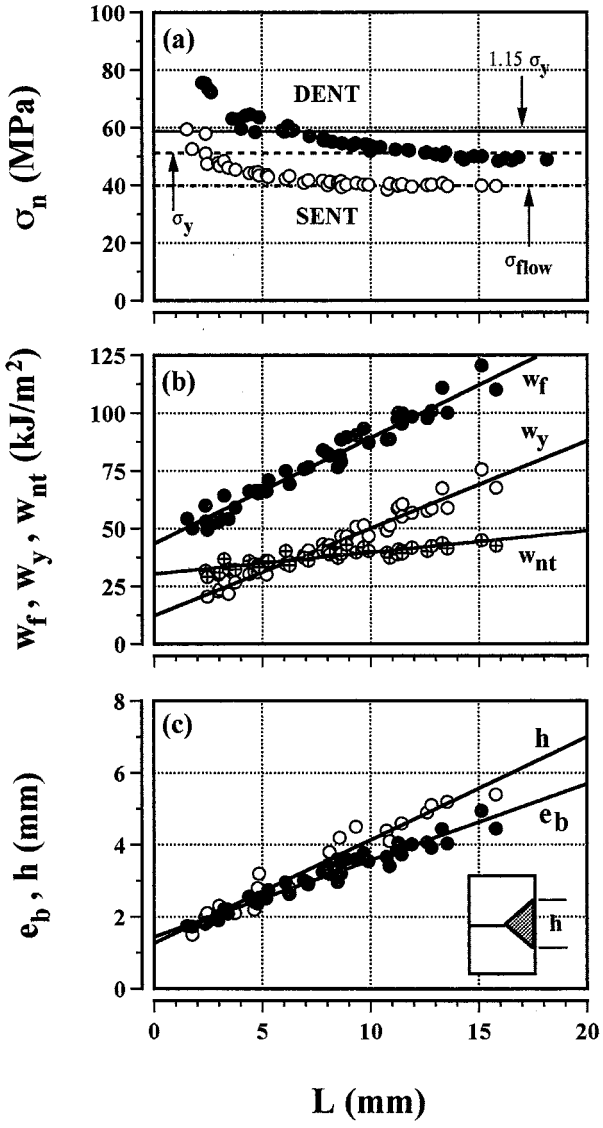

Figure 19 Plots of net-section stress, σ_n, the specific work of fracture parameters, extension to break, e_b, and the height of the plastic zone, h, versus ligament length, L, for SENT specimens at 23 °C; $W = 35$ mm, $Z = 70$ mm and $v = 5$ mm/min.

compared to a value of 0.052 for DENT specimens. This gives a plastic work done (w_p) of 32.31 MJ/m^3 for SENT compared to 62.89 MJ/m^3 for DENT specimens.

Finally, the value of specific essential work of fracture was estimated via crack opening displacement. As shown in Fig. 19c, a linear relationship is also obtained between extension to break and ligament length, for SENT specimens. The extrapolation of the best linear regression line to $L = 0$ gives a crack opening displacement value of 1.47 mm. Accordingly, w_e, was estimated using Equation 14 with $m\sigma_y \approx 0.78\sigma_y$. This estimation gave a $w_e \approx 39$ kJ/m^2 which agrees reasonably well with the value of 43.48 kJ/m^2, obtained by the direct method.

5. Summary

From the results presented in this paper on an uPVC film of thickness 0.26 mm the following conclusions were drawn:

- The specific essential works of fracture (w_e) was more or less insensitive to changes in specimen width, specimen gauge length, loading rate and temperature. The w_e value for SENT specimen was 25% higher than that of DENT specimens.
- The specific essential work terms relating to yielding ($w_{e,y}$) and necking/tearing ($w_{e,nt}$) were linear functions of the ligament length. These energy terms showed no significant variation with respect to specimen width, specimen gauge length and the loading rate. $w_{e,nt}$ was always greater than $w_{e,y}$. Whilst the latter was found to be independent of specimen geometry, the former was found to be geometry dependent, being higher for SENT geometry.
- The specific non-essential work term, βw_p, was found to be more or less insensitive to all the parameters studied here, except the geometry of the test specimen and test temperature, where a significant change in shape factor, β, was also noted. Values of βw_p and β both increased with increasing temperature, and both were significantly higher for SENT geometry. On the other hand, the non-essential work of fracture for yielding, $\beta_y w_{p,y}$, and for necking/tearing, $\beta_{nt} w_{p,nt}$, were found to be strongly affected by all the parameters studied in the present work.
- The ligament length requirement of $L \leq \min(2R_p, W/3)$ was found to be too restrictive for this polymer.
- The condition that the steady state value of net-section stress should be; $\sigma_{ns} = 1.15\sigma_y$ for DENT and $\sigma_{ns} = \sigma_y$ for SENT, was not appropriate for uPVC material. For this material, $\sigma_{ns} = \sigma_y = 1.15\sigma_{flow}$ for DENT and $\sigma_{ns} = 0.78\sigma_y = \sigma_{flow}$ for SENT.

References

1. K. B. BROBERG, *Int. J. Fract.* **4** (1968) 11.
2. B. COTTERELL and J. K. REDDEL, *Int. J. Fract.* **13** (1977) 267.
3. Y. W. MAI and B. COTTERELL, *J. Mat. Sci.* **15** (1980) 2296.
4. *Idem., Eng. Fract. Mech.* **21** (1995) 123.
5. S. HASHEMI, *Polym. Eng. Sci.* **37** (1997) 912.
6. S. HASHEMI and Z. YUAN, *Plastics, Rubber and Composites Processing and Applications* **21** (1994) 151.
7. S. HASHEMI, *J. Mat. Sci.* **28** (1993) 6178.
8. *Idem., ibid.* **32** (1997) 1573.
9. J. KARGER-KOCSIS, T. CZIGANY and E. J. MOSKALA, *Polym.* **38** (1997) 4587.
10. *Idem., ibid.* **39** (1998) 3939.
11. W. Y. F. CHAN and J. G. WILLIAMS, *Polym.* **35** (1994) 1666.
12. J. WU and Y. W. MAI, *Polym. Eng. Sci.* **36** (1996) 2275.
13. R. S. SETH, A. G. ROBERTSON, J. D. HOFFMAN and Y. W. MAI, *Tappi J.* **76** (1993) 109.
14. Y. W. MAI, H. HE, R. LEUNG and R. S. SETH, in "Int. Fract. Mech. Vol. 26 STP1256," edited by W. G. Reuter et al., (ASTM, Philadelphia, 1995) p. 587.
15. R. H. HULL, *J. Mech. Phys. Solids.* **4** (1952) 19.
16. W. D. LI, R. K. Y. LI and S. C. TJONG, *Polymer Testing.* **16** (1997) 563.

Received 18 February
and accepted 11 March 1999